Multi-color solar absorption as a synergetic UV up-conversion enhancement mechanism in LiYF 4 :Yb 3+ ,Tm 3+ nanocrystals

Bhagyesh Purohit, Yannick Guyot, David Amans, Marie-France Joubert, Benoit Mahler, Shashank Mishra, Stéphane Daniele, Christophe Dujardin, Gilles Ledoux

Multi-color solar absorption as a synergetic UV up-conversion enhancement mechanism in $LiYF_4$:Yb^{3+},Tm^{3+} nanocrystals

Bhagyesh Purohit,[†,‡] Yannick Guyot,[†] David Amans,[†] Marie-France Joubert,[†] Benoit Mahler,[†] Shashank Mishra,[‡] Stephane Daniele,[‡,¶] Christophe Dujardin,[†] and Gilles Ledoux [*,†]

†*Univ Lyon, Université Claude Bernard Lyon 1, CNRS, Institut Lumière Matière, F-69622, LYON, France*

‡*Univ Lyon, Université Claude Bernard Lyon 1, CNRS, Institut de Recherches sur l'Environnement et la Catalyse de Lyon, F-69622, LYON, France*

¶*Present address: C2P2-UMR 5265, ESCPE-Lyon, BP 2077, 69616 Villeurbanne cedex, France*

E-mail: gilles.ledoux@univ-lyon1.fr

Phone: +33 (0)4 72 44 83 38

Abstract

Motivated by the technologically important spectral conversion of sunlight for efficient photocatalysis, we present a detailed analysis of the multi-color excitation of $LiYF_4$:Yb^{3+},Tm^{3+} nanocrystals leading to UV emission through upconversion. We demonstrate in particular that the combination of blue and IR light for generating upconversion UV emission is a linear mechanism that occurs at rather low density of excitation (a few mW/cm^2). This up-conversion efficiency is fully compatible with

the broad band excitation from the sun, with comparable density similar to daylight excitation. It demonstrates that an appropriate design combining photocatalyst and dedicated up-converter leads to a drastic improvement of the photocatalytic effect.

Keywords

upconversion, photocatalysis, LiYF4, YLiF4 thulium, ytterbium

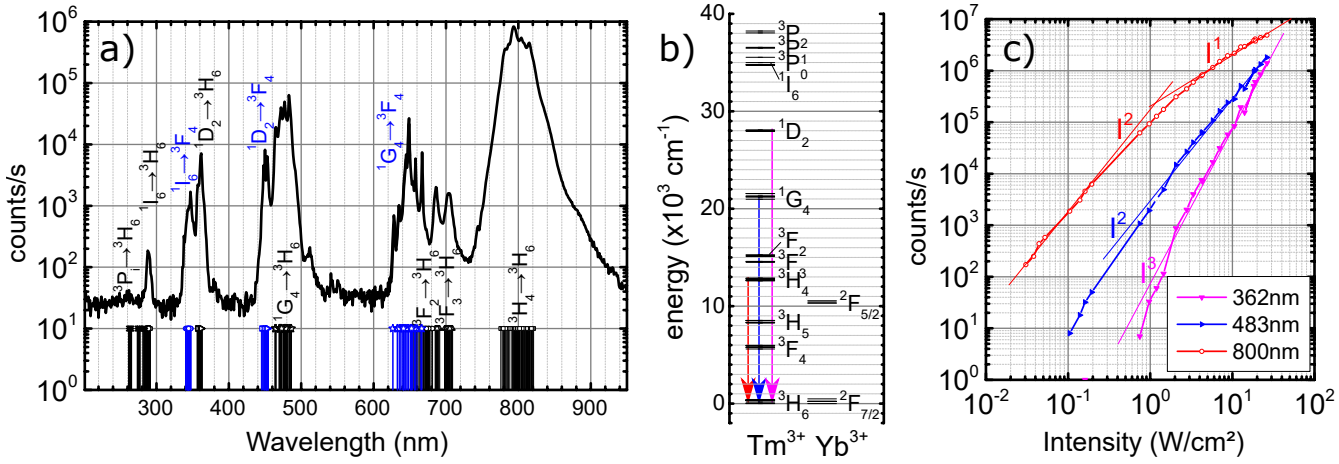

Figure 1: (a) Upconversion spectra of 20% Yb and 0.5% Tm co-doped $LiYF_4$ nanocrystals under a 973 nm excitation wavelength with an intensity of 4.32 W/cm^2. The black lines show the emission transitions going down to the ground level of Tm^{3+} ($^3H_6$) while the blue lines represent the transitions going down to the first excited multiplet of Tm^{3+} ($^3F_4$). (b) energy levels of Thullium and Ytterbium ions in $LiYF_4$ according respectively to Dulick et al[1] and to Bensalah et al.[2] The arrows indicate the three transitions presented in panel (c) with the same color code. (c) luminescence intensity variations of the principal emission components with respect to the excitation intensity of the IR laser.

Up-conversion phosphors emit higher energy photons than those absorbed. This effect is efficient in rare earth doped materials under mild irradiation conditions from mW/cm^2 to hundreds of W/cm^2. The phenomena was discovered in the late 50's by Bloembergen[3] and just a few years later Auzel showed that it could be combined with energy transfer in order to improve its efficiency.[4,5] This additional process, called APTE (*Addition de photons par transfert d'énergie*) or ETU (Energy Transfer Upconversion), was thus naturally envisioned to convert the inefficient infrared part of the solar spectrum into photons efficiently absorbed

by solar cells (see[6,7] and references therein).

Solar driven photocatalysis is a steadily growing market that reached 2 billions $ in 2014.[8] Most of the applications are based on titania but other inorganic (ZnO, CeO_2, ...), metal complexes (tetrabutylammonium decatungstate, chromium carbenes, ...) or organic compounds (acetone, ...) are also used.[8] A common trend of this photocatalysts is that they are efficient mainly under UV excitation. Therefore only a very small amount of solar spectrum photons are useful. For instance only 1.5% of solar spectrum photons are exploited in the case of titania. Using upconversion materials to convert many more solar spectrum photons into useful ones could greatly enhance the production rate, provided that they demonstrate the ability to produce UV photons. Considering the non-linearity of this effect, up-conversion enhanced photocatalysis has only been demonstrated with a relatively high excitation provided by an infrared laser.[9–15] Nevertheless, we demonstrated previously that up-converting $NaGdF_4$:Yb^{3+},Tm^{3+} nanocrystals can also enhance photocatalysis under solar irradiation.[16] This last result was counter-intuitive if one considers that the addition of the energy of at least 3 photons in the IR are required to obtain one excitation in the UV. In this paper we aim to demonstrate that the IR $\rightarrow$ UV conversion process under broadband excitation is not a third order process, with respect to the infrared at low power density excitation. Under broad band excitation, a subtle intermix of energy transfer and excited state absorption using the blue part of the solar spectrum converts it to a first order mechanism, entirely compatible with natural light excitation.

The $LiYF_4$:Yb^{3+},Tm^{3+} system is reported to be one of the most efficient ones for the generation of UV photons by upconversion.[17] Here we have synthesized it by the thermal decomposition method using anhydrous metal trifluoroacetate derivatives [$Ln(TFA)_3(DME)$] (Ln = Y, Tm, Yb) and Li(TFA)(DME) (where TFA = trifluoroacetate, and DME = dimethoxyethane) as molecular precursors (the detailled protocol is given in the supplementary information). The absence of water molecules during synthesis avoids the risk of the formation of oxofluoride phases and produces high quality nanocrystals (NCs) with enhanced upconversion

intensity. Water molecules are a well-known luminescence quencher,[18] and the synthesis of NCs with water free surfaces is mandatory. The formation of a pure phase, well-crystallized and monodisperse $LiYF_4$: 20% Yb^{3+}, 0.5% Tm^{3+} (measured at 19±1% Yb and 0.6±0.5% by EDS) NCs was confirmed by powder XRD, EDS, TEM and high resolution TEM studies (see supporting information).

The samples are placed on a heating/cooling stage DSC600 from Linkam corporation equipped with a sapphire window. They are therefore maintained at 25°C at all time. A first laser with continuous wave (CW) excitation at 973 nm and with a power of 2 W is focused to a square spot of 1×1 mm^2 on the sample with a quasi top-hat energy distribution. Its power can be varied thanks to a set of neutral density filters allowing a variation of the intensity from 200 W/cm^2 down to 8.4 $\mu W/cm^2$. A second laser, an Optical Parametric Oscillator (OPO) from EKSPLA (model NT230-50-SH) with a fixed repetition rate of 50 Hz and a pulse width of 3 ns, is also shone on the sample. Its emission wavelength can be tuned from 211 nm up to 2.5 μm. The spot size is 5 mm diameter on the sample with a Gaussian intensity distribution. The two lasers are collinear at the sample surface. Therefore in the central 1x1 mm^2 square spot both laser excitation are almost homogeneous (meaning less than 10% variation over the central 1×1 mm^2 area for both lasers). The light emitted from this central spot is collected by an optical fiber placed as close as possible to the sample and fed to a monochromator from Jobin-Yvon (TRIAX 320) equipped with automatic order removing filters and coupled to an EMCCD (Newton 920U from Andor) or a cooled photomultiplier (Hamamatsu R943-02). The signal from the photomultiplier is sent to a SR400 counting module from Stanford Research Systems. A simple LED (M455L1 from Thorlabs) can be focused on the sample over a surface of 0.6 cm^2, as an alternative to the OPO laser source excitation. The wavelength of the peak intensity of the LED has been measured to be 460nm with a FWHM of 30 nm. Its intensity can be varied continuously from 0 to 15 mW/cm^2. The emission can also be excited thanks to a Xe laser driven light source EQ99 from Energetiq together with a YG12 colored long pass filter (see figure 7 of the supplementary information)

to mimic a solar irradiation without its UV component.

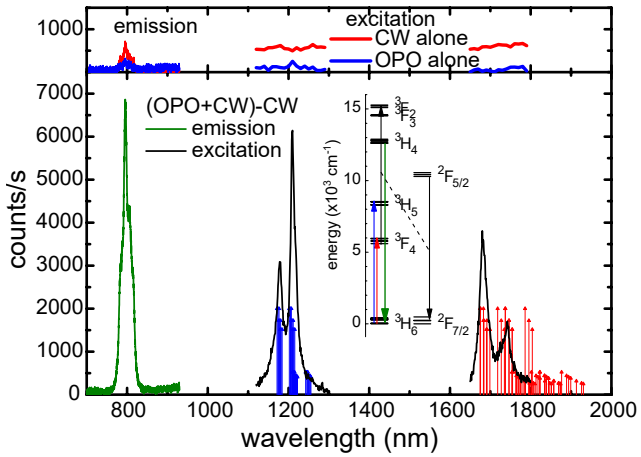

Figure 2: Upper panel: In blue excitation (right) and emission (left) of the $^3H_4 \rightarrow ^3H_6$ transition of Tm^{3+} ions in $LiYF_4$ nanocrystals at 805 nm with the OPO laser alone. In red, excitation (right) and emission (left) of the same transition with the CW laser alone. Lower panel: for the same transition in black excitation spectra under a combined excitation of a CW laser at 973 nm with an intensity of 13 mW/cm^2 and a variable wavelength OPO pulsed laser after subtraction of the IR laser contribution. On the left, in green, the corresponding emission spectra with the OPO centered at 1210 nm.

Figure 1a shows, in a semi-log scale, a characteristic upconversion emission spectrum of $LiYF_4$ nanoparticles with a doping concentration measured by EDS of 19±1% Yb^{3+} and 0.6±0.5% Tm^{3+} ions under a moderate density of excitation (4.32 W/cm^2 at 973 nm). The different emission lines can be easily ascribed to the $f - f$ intraconfigurational transitions of Thulium as reported by Dulick and collaborators[1] and for which the energy level diagram is presented in figure 1b. The spectrum is dominated by the emission around 800 nm coming from the $^3H_4 \rightarrow ^3H_6$ transition from Tm^{3+} ions. At shorter wavelength, the blue emission around 480 nm arises mainly from $^1G_4 \rightarrow ^3H_6$ and the UV region is dominated by the $^1D_2 \rightarrow ^3H_6$ transition at 360 nm. The intensity of upconversion has been compared to that of a single crystal of similar composition (see figure 3 of the supplementary information). The overall intensity of the nanoparticles under the same excitation intensity and the same collection geometry corresponds to 78% of the one measured on the single crystal. Upconversion photoluminescence Quantum yield (UC-QY) and Energy conversion efficiencies

(ECE) have also been measured and are reported in table 1 of the supplementary information. While smaller (by a factor of ∼2) than the one reported by[19] our nanoparticles are about ten times smaller than theirs. Because of the larger surface to volume ratio in our case, It suggests that our particles have only a small quenching at the surface, while they are well crystallized and exempt of volume defects.

These processes are non linear, figure 1c presents the evolution of luminescence intensity of the three main emissions as a function of the excitation source intensity. From a few tens of mW/cm^2 up to 30 W/cm^2, the blue emission shows an almost quadratic behavior, the UV emission depends on the third power of the excitation density while the 800 nm emission is quadratic up to about 1 W/cm^2 and becomes linear afterwards.

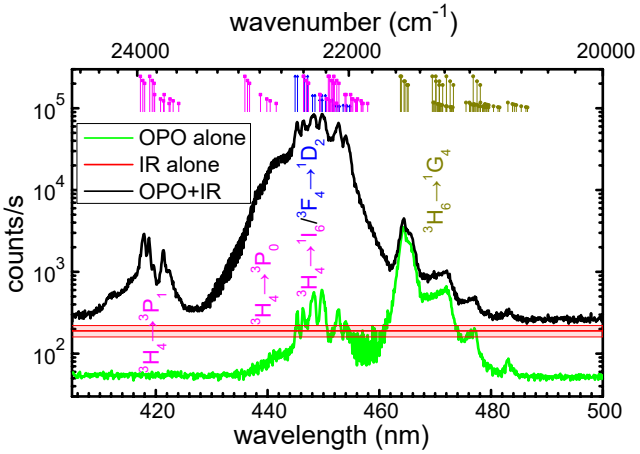

Figure 3: Excitation spectra of the $^1D_2 \rightarrow {}^3H_6$ transition of Tm^{3+} ions in $LiYF_4$:Yb,Tm nanocrystals. The black curve corresponds to the dual excitation with a CW IR laser at 973 nm and the OPO laser of varying wavelength. The green curve corresponds to the excitation spectrum using only the OPO laser source. The red curve corresponds to the average emission intensity when using only the IR excitation (the clear red band being the $\pm 2\sigma$ intensity fluctuation over time). In the upper part the different possible transitions for Thulium ions[1] are plotted with their intensities normalized to their expected relative population from the starting levels according to a simple Boltzmann distribution at room temperature. The colors of the transition being the text tag colors of the bottom figure.

The full description of the up-conversion process in co-doped Thulium-Ytterbium systems is still a matter of debate and essentially two different scenarios have been considered, both using Yb^{3+} for each excitation step: either a sequential transfer or a cooperative sensitization

by several Yb^{3+} ions. In the first hypothesis[20,21] an Yb^{3+} ion transfers its excitation to a Tm^{3+} into its $^3H_5$ and/or $^3F_4$ level. Then a second transfer promotes Tm^{3+} in a higher excited state ($^3F_2$ or even $^1G_4$) and the process is repeated as long as the excited Yb^{3+} ions can transfer some excitation. In the second hypothesis,[22,23] two excited Yb^{3+} ions which are sufficiently close to a single Tm^{3+} ion, transfer simultaneously by cooperative sensitization their excitation to the Tm^{3+} ion promoting it directly to its $^1G_4$ excited state. Then some additional excitation from another excited Yb^{3+} ion brings the Tm^{3+} to a higher excited state.

In order to provide a deeper insight into these two potential processes, we have performed excited state excitation spectroscopy. A CW IR laser at low enough excitation density (13 mW/cm^2) is used to populate the excited state of the Yb^{3+} ions without any detectable up-conversion emission. Under this excitation, we expect to have a significant amount of Yb^{3+} ions in the excited state ($\sim 2.2\times10^{15}$ cm^{-3}) at all time and a small amount of Tm^{3+} in the lower lying excited states ($^3F_4$ and $^3H_5$) excited through energy transfer from Yb^{3+} $^2F_{5/2}$ at all time. Thus, when the Tm^{3+} are brought to one of the $^3F_4$ or $^3H_5$ excited state by a second tunable laser, through energy transfer, the excited Tm^{3+} ions can be brought to higher excited states if the correct conditions exist. The $^3H_4 \rightarrow {}^3H_6$ upconversion emission at 800 nm is thus monitored as a function of the wavelength of the tunable excitation laser. As can be seen in figure 2, the 800 nm emission is hardly detected when the 2 lasers are used as separate excitation source, while a series of peak clearly appear around 1680 nm and 1210 nm when the two lasers are used simultaneously. These two excitation lines perfectly match the $^3H_6 \rightarrow {}^3F_4$ and $^3H_6 \rightarrow {}^3H_5$ transitions respectively. It indicates that when the $^3F_4$ level is populated, since the $^3F_4$ to $^3F_2$ energy difference is almost resonant with the Ytterbium $^2F_{5/2}$ to $^2F_{7/2}$ energy difference , it is an extremely efficient means of obtaining the emission from the $^3H_4$ level. To confirm this hypothesis, lifetimes in the excited state have been performed with either a single excitation of Yb^{3+} or a double excitation with a CW laser at 973nm and a pulsed laser tuned at 1210nm corresponding to the $^3H_6 \rightarrow {}^3H_5$ transition. This data is

presented in figure 4 of the supplementary information and it confirms the process described above.

A similar study has been performed on the $^1G_4 \rightarrow {}^3H_6$ emission of Tm^{3+} and the results are presented in figure 5 of the supplementary information. The main result is that the most efficient way to excite this level is by cooperative sensitization. Indeed the sequential excitation would involve a transition from $^3H_5$ to $^1G_4$ levels of Tm^{3+}, which is most unlikely since its energy correspond to 125% of the $^2F_{5/2} \rightarrow {}^2F_{7/2}$ transition in Yb^{3+}.

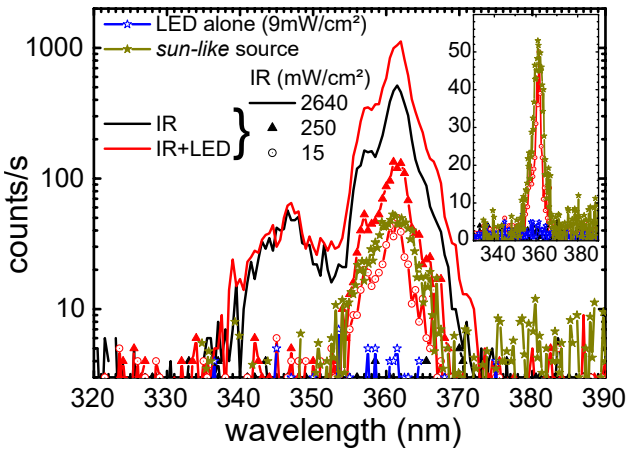

Figure 4: Emission spectra of Tm^{3+} ions in $LiYF_4$:Yb,Tm nanocrystals under dual excitation (red lines) of a SCW IR laser at 973 nm and the LED or by the LED alone (blue stars) or the IR laser alone (black lines) . The brown stars correspond to an excitation with a *sun-like* excitation (lamp +filter). The inset is a close-up in linear scale of the weaker spectra. The noise of the detector is around 3 counts/s.

More interesting is the study of the $^1D_2$ to $^3H_6$ transition around 360 nm. As shown in figure 6 of the supplementary information, increasing the IR laser excitation density up to 100 mW/cm^2 results in weak emission from the $^3H_4$ and the $^1G_4$, and undetectable from $^1D_2$. When excited at about 450 nm with a pulsed laser fluence of 50 mJ/cm^2, this emission cannot be detected either. When the lasers are combined, a strong synergetic effect is demonstrated with an increase by more than 2 orders of magnitude of the $^1D_2 \rightarrow {}^3H_6$ emission at 360 nm. The excitation spectrum of this phenomenon is presented in figure 3 where the different transitions can be clearly assigned. It demonstrates that excited state absorption from the $^3F_4$ to the $^1D_2$ or from the $^3H_4$ level to the $^1I_6$ or ^3P_i levels are very efficient processes,

leading to a drastic increase of the emission of the $^1D_2$ level when the IR source helps to populate the $^3F_4$ level thanks to an energy transfer from the Yb^{3+} $^2F_{5/2}$ level. On the other hand, there is no effect on the $^1D_2$ emission with the addition of the IR source when the OPO source leads to a population of the $^1G_4$ level (direct excitation from the $^3H_6$). This means that an energy transfer from the Yb^{3+} $^2F_{5/2}$ level is not efficient for populating the $^1D_2$ level from the $^1G_4$ level. These results allow us to state that the most efficient processes leading to the excitation of the $^1D_2$ by classical upconversion are the sequential mechanisms involving a first step that populates the $^3F_4$ level and then a second step of cooperative sensitization from two excited Yb^{3+} ions to generate a $^1D_2$ excited Tm^{3+} ion. This result is consistent with the calculations of Carnall et al.[24] who showed that the $^3F_4 \rightarrow {}^1D_2$ transition is hypersensitive (ΔJ=2) and its squared U(2) matrix element is 0.5689, therefore one of the strongest absorption of the Tm^{3+} ions. Again lifetime in the excited state has been measured under single or dual excitation and the results are presented in figure 7 of the supplementary information. As before this confirms the above described process with the appearance of a single monoexponential decay for the $^1D_2 \rightarrow {}^3H_6$ emission once the second laser is present corresponding only to the lifetime of the $^1D_2$ level.

These results were obtained with relatively high excitation densities far from day light excitation. It allows an understanding of the different steps that can take place in the upconversion phenomena and for us to sort out which wavelength domains play a role in a broadband excitation scheme. However, by our own admission, it is far from real life applications like a solar photocatalysis plant. In the following section, we aim to demonstrate that this process still occurs under continuous moderate sunlight-type excitation conditions. The OPO laser is replaced by the standard LED as described before, that has its maximum in the range of the $^3F_4 \rightarrow {}^1D_2$ excitation. Figure 4 presents spectra in the range of the $^1D_2 \rightarrow {}^3H_6$ emission under separate and simultaneous blue and IR excitations highlighting the same synergetic phenomena. These excitations correspond to a typical sun irradiance on the earth for these two ranges of wavelengths as described by the standard AM1.5.[25] As

can be seen in this figure as soon as the IR intensity is decreased below a few W/cm^2 no UV light can be detected if no blue excitation is present. On the contrary, if the blue LED is turned on with rather low excitation intensities (9mW/cm^2) UV emission can be detected even for very low intensities of the IR laser.

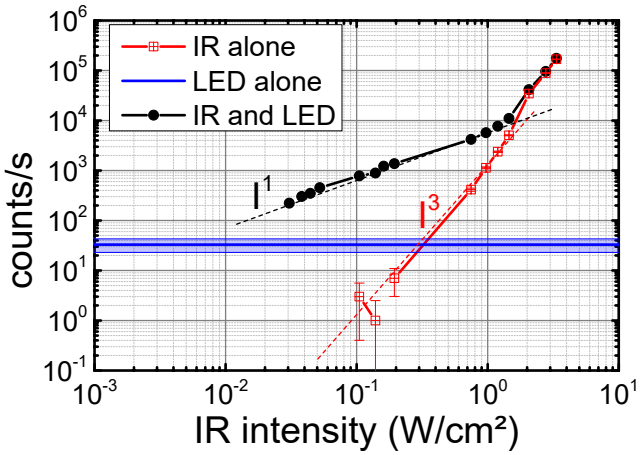

Figure 5: total emission in the range 360-370 nm Tm^{3+} ions in $LiYF_4$:Yb,Tm nanocrystals under dual excitation (black line) of a CW IR laser at 973 nm and a LED centered at 460 nm. Excitation of the CW IR laser (red) alone or the LED alone (blue line together with its $\pm 2\sigma$ variation) as a function of the IR intensity. The LED is kept at 3 mW/cm^2. The dashed lines are guide for the eyes showing a variation following a linear relation with intensity (black) or following a power law with a factor of 3 (red).

In order to demonstrate the impact of the discussed mechanisms on the change of power law regime for the $^1D_2$ emission, we compared the UV intensity as a function of the IR laser intensity with or without the blue LED (3 mW/cm^2). The results presented in Figure 5 with IR excitation alone follow a third order dependence as expected and already presented. When the LED is turned on, the power law shape is radically modified and becomes linear up to 1 W/cm^2 indicating that the IR excitation switches from a three photon to a single IR photon process. As described above, by energy transfer, the IR absorption of a single photon in Yb^{3+} allows the excitation of the $^3F_4$ of Tm^{3+}, and the blue excitation promotes Tm^{3+} to the $^1D_2$ state. At higher excitation density, the third order process is, as expected, dominant. Similarly, when varying the power of the LED while keeping the IR laser power constant, a linear behavior is observed as evidenced in figure 8 of the supplementary information. It

demonstrates that the overall mechanism involves 1 photon in the blue and 1 photon in the IR, which satisfies the energy conservation law to obtain UV light at 360 nm.

As a last demonstration, we simulated a solar illumination using a filtered Xe lamp with a spectrum shown in figure 9 of the supplementary information. UV emission under such excitation is presented in figure 4 as brown stars compared to the IR excitation through up-conversion mechanisms or with the combination of LED and IR laser. A clear band is obtained at 360 nm and the band is slightly broader because the system resolution in this case was 2.5 nm instead of 1 nm.

This excitation, similar to the sun, is able to promote high energy excitations in Yb^{3+},Tm^{3+} co-doped $LiYF_4$. It would enable the generation, by energy transfer, of electron-hole pairs compatible with standard photocatalysts. Combining up-converter and photocatalyst, a significant part of the solar spectrum that is unused can stimulate photocatalysis, which, after optimization and use of efficient energy transfer ions[26–28] has the potential to improve the overall photocatalysis efficiency by a factor of 3 as we have shown in a previous work.[16] Such an approach would allow a significant decrease in the time of reaction that currently take between hours and weeks in solar photocatalysis plants[8] and could also allow the use of photocatalysts that have been discarded since they need photons with an energy that is too high.

This exciting result comes from the simple addition of the energy of an IR and a visible photon, thus reducing the non-linearity of the UV upconversion phenomena, which in part originates from the idea behind Auzel's original publication in 1966 to make a "quantum counter by energy transfer from Yb^{3+} to Tm^{3+}".[5]

Acknowledgement

The authors acknowledge the funding from Agence Nationale de la Recherche through the grant number ANR-17-CE09-0002.

References

(1) Dulick, M.; Faulkner, G.; Cockroft, N.; Nguyen, D. Spectroscopy and dynamics of upconversion in Tm^{3+}: $YLiF_4$. *Journal of Luminescence* **1991**, *48-49*, 517–521.

(2) Bensalah, A.; Guyot, Y.; Ito, M.; Brenier, A.; Sato, H.; Fukuda, T.; Boulon, G. Growth of Yb^{3+}-doped $YLiF_4$ laser crystal by the Czochralski method. Attempt of Yb^{3+} energy level assignment and estimation of the laser potentiality. *Optical Materials* **2004**, *26*, 375–383.

(3) Bloembergen, N. Solid state infrared quantum counters. *Physical Review Letters* **1959**, *2*, 84.

(4) Auzel, F. Compteur quantique par transfert d'énergie entre deux ions de terres rares dans un tungstate mixte et dans un verre. *Comptes rendus de l'académie des sciences de Paris* **1966**, *262*, 1016.

(5) Auzel, F. Compteur quantique par transfert d'énergie de Yb3+ à Tm3+ dans un tungstate mixte et dans un verre germanate. *Comptes rendus de l'académie des sciences de Paris* **1966**, *263*, 819.

(6) van Sark, W. G.; de Wild, J.; Rath, J. K.; Meijerink, A.; Schropp, R. E. Upconversion in solar cells. *Nanoscale research letters* **2013**, *8*, 81.

(7) Yang, W.; Li, X.; Chi, D.; Zhang, H.; Liu, X. Lanthanide-doped upconversion materials: emerging applications for photovoltaics and photocatalysis. *Nanotechnology* **2014**, *25*, 482001.

(8) Spasiano, D.; Marotta, R.; Malato, S.; Fernandez-Ibañez, P.; Di Somma, I. Solar photocatalysis: Materials, reactors, some commercial, and pre-industrialized applications. A comprehensive approach. *Applied Catalysis B: Environmental* **2015**, *170-171*, 90–123.

(9) Tang, Y.; Di, W.; Zhai, X.; Yang, R.; Qin, W. NIR-Responsive Photocatalytic Activity and Mechanism of $NaYF_4$:Yb,Tm@TiO_2 Core–Shell Nanoparticles. *ACS Catalysis* **2013**, *3*, 405–412.

(10) Zhang, Y.; Hong, Z. Synthesis of lanthanide-doped $NaYF_4$@TiO_2 core–shell composites with highly crystalline and tunable TiO_2 shells under mild conditions and their upconversion-based photocatalysis. *Nanoscale* **2013**, *5*, 8930.

(11) Wang, W.; Ding, M.; Lu, C.; Ni, Y.; Xu, Z. A study on upconversion UV-vis-NIR responsive photocatalytic activity and mechanisms of hexagonal phase $NaYF_4$:Yb^{3+},Tm^{3+}@TiO_2 core-shell structured photocatalyst. *Applied Catalysis B: Environmental* **2014**, *144*, 379–385.

(12) Wang, W.; Li, Y.; Kang, Z.; Wang, F.; Yu, J. C. A NIR-driven photocatalyst based on α-$NaYF_4$:Yb,Tm@TiO_2 core–shell structure supported on reduced graphene oxide. *Applied Catalysis B: Environmental* **2016**, *182*, 184–192.

(13) Ullah, S.; Hazra, C.; Ferreira-Neto, E. P.; Silva, T. C.; Rodrigues-Filho, U. P.; Ribeiro, S. J. L. Microwave-assisted synthesis of NaYF $_4$:Yb^{3+}/Tm^{3+} upconversion particles with tailored morphology and phase for the design of UV/NIR-active $NaYF_4$:Yb^{3+}/Tm $^{3+}$@TiO_2 core@shell photocatalysts. *CrystEngComm* **2017**, *19*, 3465–3475.

(14) Su, W.; Zheng, M.; Li, L.; Wang, K.; Qiao, R.; Zhong, Y.; Hu, Y.; Li, Z. Directly coat TiO 2 on hydrophobic NaYF4 :Yb,Tm nanoplates and regulate their photocatalytic activities with the core size. *Journal of Materials Chemistry A* **2014**, *2*, 13486.

(15) Yin, D.; Zhang, L.; Cao, X.; Tang, J.; Huang, W.; Han, Y.; Liu, Y.; Zhang, T.; Wu, M. Improving photocatalytic activity by combining upconversion nanocrystals and Mo-doping: a case study on β-NaLuF $_4$:Gd,Yb,Tm@SiO $_2$ @TiO $_2$:Mo. *RSC Adv.* **2015**, *5*, 87251–87258.

(16) Chen, Y.; Mishra, S.; Ledoux, G.; Jeanneau, E.; Daniel, M.; Zhang, J.; Daniele, S. Direct Synthesis of Hexagonal $NaGdF_4$ Nanocrystals from a Single-Source Precursor: Upconverting $NaGdF_4$:Yb^{3+},Tm^{3+} and Its Composites with TiO_2 for Near-IR-Driven Photocatalysis. *Chemistry - An Asian Journal* **2014**, *9*, 2415–2421.

(17) Mahalingam, V.; Vetrone, F.; Naccache, R.; Speghini, A.; Capobianco, J. A. Colloidal Tm^{3+}/Yb^{3+}-Doped $LiYF_4$ Nanocrystals: Multiple Luminescence Spanning the UV to NIR Regions via Low-Energy Excitation. *Advanced Materials* **2009**, *21*, 4025–4028.

(18) Rabouw, F. T.; Prins, P. T.; Villanueva-Delgado, P.; Castelijns, M.; Geitenbeek, R. G.; Meijerink, A. Quenching Pathways in $NaYF_4$:Er^{3+},Yb^{3+} Upconversion Nanocrystals. *ACS Nano* **2018**, *12*, 4812–4823.

(19) Meijer, M. S.; Rojas-Gutierrez, P. A.; Busko, D.; Howard, I. A.; Frenzel, F.; Würth, C.; Resch-Genger, U.; Richards, B. S.; Turshatov, A.; Capobianco, J. A.; Bonnet, S. Absolute upconversion quantum yields of blue-emitting $LiYF_4$:Yb^{3+},Tm^{3+} upconverting nanoparticles. *Physical Chemistry Chemical Physics* **2018**, *20*, 22556–22562.

(20) Guy, S.; Jurdyc, A.; Jacquier, B.; Meffre, W. Excited states Tm spectroscopy in ZBLAN glass for S-band amplifier. *Optics Communications* **2005**, *250*, 344–354.

(21) Peretti, R.; Jurdyc, A.-M.; Jacquier, B.; Gonnet, C.; Pastouret, A.; Cavani, O. How do traces of thulium explain photodarkening in Yb doped fibers? **2010**, 6.

(22) Knüpfer, A.; Ostroumov, V.; Heumann, E.; Huber, G.; Lupei, V. Mechanisms of upconversion excitation of blue emission in YAG:Tm, Yb. *Le Journal de Physique IV* **1994**, *04*, C4–501–C4–504.

(23) Mishra, S.; Ledoux, G.; Jeanneau, E.; Daniele, S.; Joubert, M.-F. Novel heterometal-organic complexes as first single source precursors for up-converting $NaY(Ln)F_4$ (Ln = Yb, Er, Tm) nanomaterials. *Dalton Trans.* **2012**, *41*, 1490–1502.

(24) Carnall, W. T.; Crosswhite, H.; Crosswhite, H. M. *Energy level structure and transition probabilities in the spectra of the trivalent lanthanides in* LaF_3; 1978; pp ANL–78–XX–95, 6417825.

(25) G173-03, A. Standard Tables for Reference Solar Spectral Irradiances: Direct Normal and Hemispherical on 37° Tilted Surface.

(26) Wang, F.; Deng, R.; Wang, J.; Wang, Q.; Han, Y.; Zhu, H.; Chen, X.; Liu, X. Tuning upconversion through energy migration in core–shell nanoparticles. *Nature Materials* **2011**, *10*, 968–973.

(27) Su, Q.; Han, S.; Xie, X.; Zhu, H.; Chen, H.; Chen, C.-K.; Liu, R.-S.; Chen, X.; Wang, F.; Liu, X. The Effect of Surface Coating on Energy Migration-Mediated Upconversion. *Journal of the American Chemical Society* **2012**, *134*, 20849–20857.

(28) Ledoux, G.; Amans, D.; Joubert, M.-F.; Mahler, B.; Mishra, S.; Daniele, S.; Dujardin, C. Modeling Energy Migration for Upconversion Materials. *The Journal of Physical Chemistry C* **2018**, *122*, 888–893.

Supporting Information Available

- synthesis and characterization of the nanoparticles;
- upconversion of the nanocrystals compared to a single crystal;
- upconversion quantum yield measurements and results;
- excitation in the excited state for the $^1G_4 \rightarrow {}^3H_6$ emission;
- lifetime in the excited state $^3H_4 \rightarrow {}^3H_6$;
- emission spectra of the $^1D_2 \rightarrow {}^3H_6$;

- lifetime in the excited state $^1D_2 \rightarrow {}^3H_6$;
- power dependency of the $^1D_2 \rightarrow {}^3H_6$ with respect to visible diode intensity;
- measured spectra of the *sun-like* lamp used.

Graphical TOC Entry